Fabrication, modeling, and evaluation of a digital output tilt sensor with conductive microspheres

Article (Accepted Version)

Fabrication, modeling and evaluation of a digital output tilt sensor with conductive microspheres

Lars Büthe, *Student Member, IEEE,* Christian Vogt, *Student Member, IEEE,* Luisa Petti, *Student Member, IEEE,* Giuseppe Cantarella, Niko Münzenrieder, *Member, IEEE,* and Gerhard Tröster, *Senior Member, IEEE*

***Abstract*—Recent advances in wearable computing ask for bendable and conformable electronic circuits and sensors, allowing an easy integration into everyday life objects. Here, we present a novel flexible tilt sensor on plastic using conductive microspheres as gravity sensitive pendulum. The sensor provides a digital output of the measurement signal without the need for any additional electronics (e.g. amplifiers) close to the sensing structure. The sensor is fabricated on a free-standing polyimide foil with SU-8 photoresist defining the cavity for the pendulum. The pendulum consists of freely movable conductive microspheres which, depending on the sense of gravity, connect different electric contacts patterned on the polyimide foil. We develop a model of the sensor and identify the amount of microspheres as one of the key parameters in the sensor design which influences the performance of the sensor. The presented tilt sensor with eight contacts achieves an angular resolution of 22.5° with a hysteresis of 10° and less at a tilt of the sensor plane of 50°. Analysis of the microsphere movements reveals a response time of the sensor at $\sim 50\,\mathrm{ms}$.**

***Index Terms*—Flexible electronics, inclinometer, microspheres, tilt sensor.**

I. Introduction

THE market of wearable electronics is currently growing at a double-digit percentage [1] as people are getting increasingly accustomed to using electronics as supporting tools in their daily life. With numerous wearables already being commercially available, the goal is now to integrate these devices into personal equipment, e.g. clothing, instead of having to wear additional devices such as smart watches. Smart textiles cover this need, as electronic components are combined with textiles. This allows a complete integration of functionality into fashion [2]. In order to not change the properties of the fabric, research is therefore focusing on the design and fabrication of mechanically flexible electronic devices. Devices like transistors have already been fabricated on flexible substrates, showing functionality down to bending radii of a few millimeters [3], [4].

As many wearables also require input from physiological data, flexible sensors are required to capture these body functions in an unobtrusive way. Recent work has already successfully investigated bendable sensors for temperature [5], pressure [6] or gas [7] signals.

An earlier version of this paper was presented at the IEEE Sensors 2015 conference and was published in its proceedings: http://dx.doi.org/10.1109/ICSENS.2015.7370308

L. Büthe, C. Vogt, G. Cantarella, L. Petti and G. Tröster are with the Electronics Laboratory, ETH Zurich, 8092 Zurich, Switzerland; e-mail: lars.buethe@ife.ee.ethz.ch

N. Münzenrieder is with the Sensor Technology Research Center, University of Sussex, Brighton, BN1 9QT, UK

Tilt measurement is ubiquitous for applications such as activity recognition or body posture detection. Accelerometers as well as tilt sensors fulfill this task. Research has already presented the integration of rigid, off-the-shelf accelerometers into a shirt for body posture detection [8]. The accelerometers simply act as tilt sensors that detect the orientation of the devices with respect to gravity. Capacitive accelerometers have also been fabricated on flexible polyimide substrate and demonstrated successfully [9].

Tilt sensors usually benefit from a less complex design and fabrication process compared to accelerometers. The pendulum, i.e. the material that responds to changes in the orientation of gravity, is one way to classify current tilt sensors: solid pendulum [10], liquid pendulum [11] and gaseous pendulum [12] sensors. The methods for detecting the current state of the pendulum are wide-spread and include resistive [13], capacitive [14], inductive [15], optical [16], fiber optic [17] and magnetic [18] measurements. In previous work, we have already demonstrated a tilt switch based on a resistive measurement principle [19].

Here, we introduce a tilt sensor which is fabricated on a flexible polyimide foil. Compared to other state-of-the-art tilt sensors, our sensor is flat and flexible. We employ a resistive measurement principle to determine the location of the pendulum inside the cavity with contact pads which are arranged in a circular array. As a pendulum, solid conductive microspheres are used that follow the orientation of gravity. The cavity is defined by SU-8 photoresist in a pillar design. The planar technology and the resulting flatness of the sensor together with the sensing principle allow integration into objects and application areas that have not be accessible with tilt sensors before.

We will present the idea of the sensing principle of the tilt sensor to achieve a digital output, followed by the fabrication process for the microspheres and the sensor itself. Subsequently, we introduce a new model of the sensor to investigate the importance of different design parameters. Finally, the static and dynamic behavior of a sample sensor is characterized.

II. Principle of operation

The sensor presented in this paper is based on conductive microspheres that act as a pendulum and follow the orientation of gravity. The cavity in which the microspheres are enclosed is of cylindrical shape defined by SU-8 pillars. Metal contact pads on the floor of the cavity act as the sensing structure to

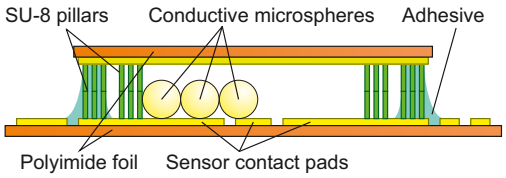

Fig. 1. Lateral view of tilt sensor structure

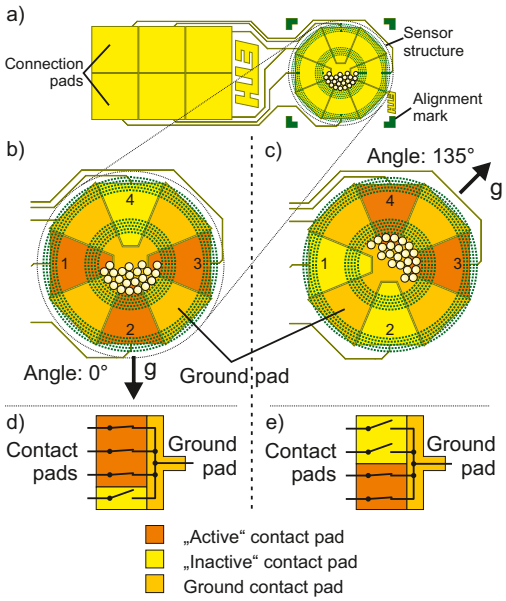

Fig. 2. Sensing principle of tilt sensor

identify the position of the microspheres. The lateral view of the proposed tilt sensor is depicted in Fig. 1.

As shown in the top view of the sensor in Fig. 2a, the sensor structure consists of circular arranged contact pads, similar to work presented by Constandinou et al. [10]. The inner ring of SU-8 pillars on top of the contact pads defines the movement area of the microspheres, whereas the outer ring is used for permanent closure of the cavity with adhesive. In between the contact pads, a ground pad fills the remaining area. An almost complete coverage of the substrate surface with a conductive layer is necessary in order to mitigate any electrostatic charges which might build up in the polyimide foil during the fabrication process and would hinder the free movement of the microspheres.

Depending on the orientation of the sensor structure with respect to gravity, the conductive microspheres create an electrical connection between the ground pad and the respective contact pads (Fig. 2b, c). These connected pads are defined as *active* (1), whereas the other pads remain *inactive* (0) having no electrical connection. By measuring the resistance between the ground pad and each contact pad, a readout of the sensor can be achieved, leading to a digital output signal. This can be represented in an equivalent electrical circuit where each contact pad can be shown as a switch which is either closed (active) or open (inactive) (Fig. 2d, e). As solely the fact whether the electrical connection is open or closed is of interest for the sensor state evaluation, the readout is independent of parasitic effects, such as resistance of connection lines.

TABLE I
POSSIBLE STEADY STATES (0: INACTIVE CONTACT PAD; 1: ACTIVE CONTACT PAD) OF A 4-CONTACT TILT SENSOR (CAVITY IS FILLED HALF WITH MICROSPHERES) WITH THE CORRESPONDING OUTPUT ANGLE

Contact number				Angle	
1	2	3	4	Limits	Output
1	1	1	0	$-22.5°$ ($337.5°$) to $22.5°$	$0°$
0	1	1	0	$22.5°$ to $67.5°$	$45°$
0	1	1	1	$67.5°$ to $112.5°$	$90°$
0	0	1	1	$112.5°$ to $157.5°$	$135°$
1	0	1	1	$157.5°$ to $202.5°$	$180°$
1	0	0	1	$202.5°$ to $247.5°$	$225°$
1	1	0	1	$247.5°$ to $292.5°$	$270°$
1	1	0	0	$292.5°$ to $337.5°$	$315°$

Applying this sensing principle, the number of contact pads has direct influence on the resolution of the tilt sensor, as discussed in more detail in section IV. Fig. 2 shows the sensor design with four contact pads as an example. The sensor design is compatible with any arbitrary number of contact pads $N \geq 3$, i.e. allowing an easy design of the sensor according to the desired requirements (e.g. resolution, size, sensitivity).

In the exemplary case of a 4-contact tilt sensor with a sufficient amount of microspheres (see section IV) in the cavity, either two or three contact pads are active at any given time (see Fig. 2b, c). This means that a total of eight different steady states can be distinguished, achieving a resolution of $45°$. Table I lists all different combinations of states of the contact pads and the corresponding angles of the 4-contact sensor and can be used to determine the orientation of the tilt sensor from the measured states of each contact pad.

III. TECHNOLOGY AND FABRICATION

We discuss the use of microspheres as the pendulum of the tilt sensor and present the fabrication process.

A. Pendulum

As a pendulum for the proposed sensing principle, different types of materials are possible: liquids as well as solids. In the category of liquids, ionic liquids (IL) seem to be the most promising ones, as they are conductive, have a high surface tension [20] and a low vapor pressure [21]. However, in a flat sensor where the height is significantly smaller than the diameter, the liquid has a large contact area with the substrate surface. Due to inter-molecular forces between pendulum and substrate surface, the large contact area causes a large hysteresis and decreases the performance of the sensor. Instead, if solids are used in the form of microspheres, the large contact area is mitigated and a higher accuracy of the sensor is achieved. In addition, a generally higher specific weight of solids compared to liquids reduces the influence of parasitic effects like friction or electrostatic forces and ensures a domination of the gravitational field on the movement of the solids.

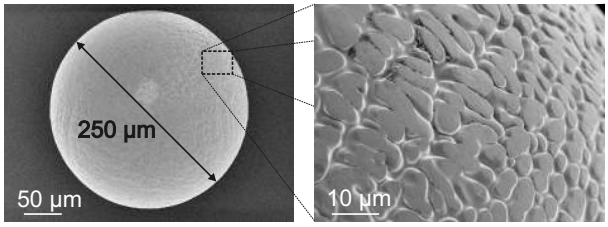

Fig. 3. SEM picture of the solder sphere with a diameter of 250 µm.

Here we use commercially available solder spheres as a solid pendulum for the tilt sensor. The solder spheres (Profound Material SAC305/250) have a diameter of $d_{sphere} = 250\,\mu\mathrm{m}$, consist of a tin, silver and copper alloy and are usually used for the soldering of ball-grid arrays [22]. Therefore, the solder spheres are cheap and readily available. They have a good uniformity in diameter ($\pm 10\,\mu\mathrm{m}$) as well as a high specific weight ($7.4\,\mathrm{g\,cm^{-3}}$) compared to other conductive microspheres such as coated hollow glass spheres [23], [24]. Fig. 3 shows an SEM image of one solder sphere which has a high sphericity. It is visible from the image, especially the inset, that the surface of the microsphere is not smooth, but has a roughness with a depth of around $1\,\mu\mathrm{m}$ and size of several micrometer. This roughness originates from the fabrication process of the solder spheres [25]. It is beneficial for the movement of the microspheres as it reduces the contact area with the substrate surface and consequently the adhesion forces.

Prior to their use in the tilt sensor, the microspheres receive an additional coating. To achieve a uniform coating a vibration device keeps them agitated during the sputter process. The vibration device consists of a loudspeaker and a battery power supply which allows an operation inside the sputter vacuum chamber. Bearing in mind the movement of the microspheres during the process, a $2\,\mathrm{nm}$ adhesion layer of nickel and subsequently a $10\,\mathrm{nm}$ gold layer are deposited. The coating increases the surface conductivity of the microsphere, as the solder tin forms an oxidation layer when in contact with air which prevents a reliable electrical contact.

The ohmic resistance of the coated microsphere is evaluated and compared to the uncoated microsphere. For this, two gold plates are placed perpendicular to each other, without creating an electrical contact. A single microsphere is placed inside this V-shaped trench, touching and connecting both plates. The resulting resistance between the two plates is measured while the pressure of the microsphere onto the plates is created solely by its own weight. While an uncoated microsphere exhibits a resistance which exceeds the $\mathrm{M\Omega}$ range, a coated microsphere shows a resistance of around $400\,\Omega$ with a standard deviation of $55\,\Omega$. Thus, the coating of the microsphere mitigates the surface oxidation and lowers the surface resistance of the microsphere.

B. Cavity

The tilt sensor is fabricated with clean room processes on a free-standing polyimide foil at process temperatures below $200\,^{\circ}\mathrm{C}$. The complete fabrication process is depicted in Fig. 4.

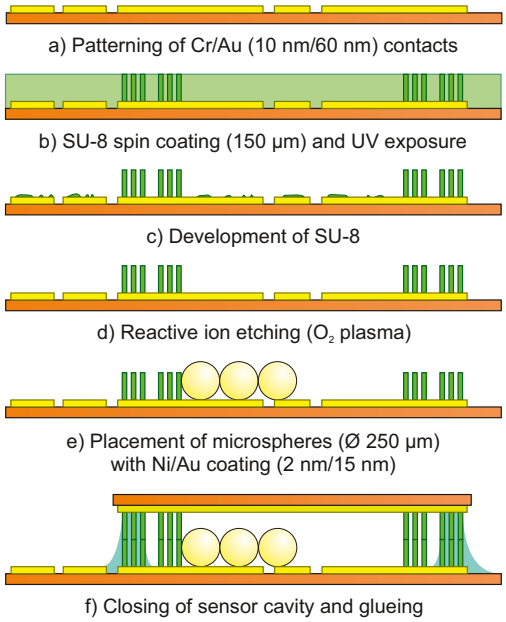

Fig. 4. Schematic fabrication flow of sensor fabricated on a free-standing polyimide foil with a maximum process temperature of $200\,^{\circ}\mathrm{C}$.

As a substrate, a $50\,\mu\mathrm{m}$-thick polyimide foil, Kapton E from *DuPont*, is used. First, a layer of $10\,\mathrm{nm}$ of chrome is deposited via e-beam evaporation, followed by $60\,\mathrm{nm}$ of gold. The chrome acts as an adhesion layer between the polyimide and the gold layer. The gold layer itself acts as the conductive electrode material. The two metal layers are then structured by wet etching. They form the electrical contact pads and the ground pad of the sensor (Fig. 4a). The break between the pad areas is $40\,\mu\mathrm{m}$. As the microspheres are in contact with each other and thus always have an electrical connection to a contact or ground pad, electrostatic forces from the polyimide are mitigated and do not influence the microsphere movement.

Subsequently, SU-8 2100 is spin coated with a thickness of $150\,\mu\mathrm{m}$ onto the substrate and structured via photolithography (Fig. 4b). The SU-8 acts on the one hand as a spacer between the bottom and top layer of the sensor and also defines the side walls of the cavity for the microspheres. The pillar design is necessary to balance the arising strain on the flexible substrate due to different thermal expansion coefficients of polyimide and SU-8. A compact ring of SU-8 instead of the pillar structure would lead to a delamination of the SU-8 from the substrate and would also decrease the bendability of the sensor. The pillars have an edge length of $60\,\mu\mathrm{m}$ and a spacing of $40\,\mu\mathrm{m}$. The SU-8 is then developed with mr-Dev 600, resulting in the desired cavity structure (Fig. 4c). To achieve a clean surface which is needed for a reliable electrical contact, reactive ion etching with an O_2-plasma is performed to remove any remaining residue from the development (Fig. 4d). The sensor design is based on two rings of five rows of SU-8 pillars where the inner ring defines the movement area for the microspheres and the outer ring is used for the sealing of the sensor.

The cavity is then filled with desired amount of microspheres which act as the pendulum (Fig. 4e). To close the

cavity, a second sheet of polyimide foil covered with a chrome/gold layer and with SU-8 pillars is placed upside down on the top of the structure and finally sealed with epoxy adhesive (Fig. 4f). These final steps are performed manually under the microscope which reduces the alignment accuracy. However, placement of the microspheres and the top layer of polyimide could also be performed fully automated to achieve an improved alignment.

The use of solder spheres limits the fabrication temperature to a maximum of 200 °C, as the solder alloy melts at around 220 °C. Reflow soldering of a packaged tilt sensor to a PCB is therefore not possible, instead conductive epoxy is a suitable alternative for creating an electrical connection.

IV. Sensor Modeling

For the first time, we now introduce a comprehensive model which provides a detailed understanding on the influence of design changes of the tilt sensor.

The above described sensor design in Fig. 2 entails different geometrical design parameters that have an influence on the sensor characteristics. Understanding the influence of these parameters allows a sensor design based on the desired resolution and linearity. The following parameters will be investigated and are visualized in Fig. 5:

1) *Number of contact pads* N: The number of contact pads inside the cavity (Fig. 5a).
2) *Sensor pad design*: Different designs are possible for the design of the sensor contact pads inside the cavity. Here, we evaluate three different arrangements (Fig. 5b):
   - *Trapezoidal*: Trapezoidal contact pads alternating with a ground plane.
   - *No ground*: Trapezoidal contact pads with no ground plane in between the pads.
   - *Rectangular*: Rectangular contact pads alternating with a ground plane.
3) *Inner contact radius* $r_{contact}$: The inner radius of the contact pads, i.e. the distance of the contact pads from the sensor center (Fig. 5c).
4) *Radius of sensor cavity* r_{cavity}: The inner radius of the sensor cavity defining the movement area of the pendulum (Fig. 5d).
5) *Ratio of ground to contact pad* η_{pad}: The ratio of the angle of the contact pad in relation to the ground pad (Fig. 5e), applicable for pad styles *Trapezoidal* and *Rectangular*. The larger the value of η_{pad}, the larger the contact pads are, where $0 \leq \eta_{pad} \leq 2$.
6) *Amount of microspheres* $N_{spheres}$: The amount of microspheres inside the cavity, determining how many contact pads are connected at a given point in time. We simplify the bulk of microspheres for the static case as a continuum, a single half-round disk with the height h_{disk} (measured from the lower part of the cavity) (Fig. 5f).

The tilt sensor is an analog-to-digital converter (ADC) which converts an analog input - the applied tilt - into a digital output - the 0 and 1 of the contact pad states. We use the quantization steps as well as the non-linearity of the ADC as performance measures for the tilt sensor [26]. The quantization

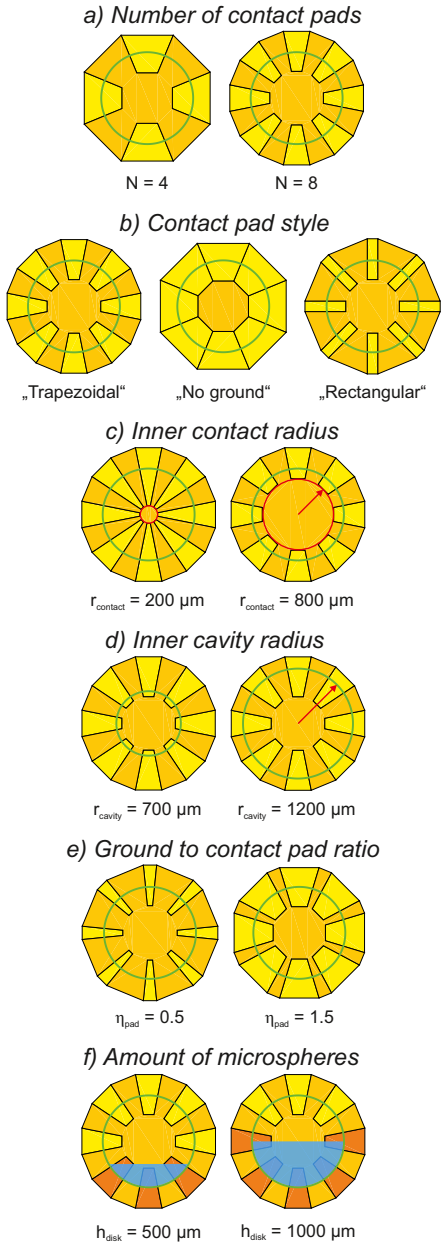

Fig. 5. Schematic representation of the different geometrical sensor parameters of the tilt sensor.

steps relate to the angular resolution α_{res} of the sensor which can be calculated according to

$$\alpha_{res} = \frac{360°}{2 \cdot N} \quad \forall N \geq 3 \tag{1}$$

where N stands for the number of contact pads.

The non-linearity describes a difference in step length in the transfer function of the ADC. Ideally all steps should have the same length. Therefore, we introduce the evaluation parameter ξ_{states} which captures the differences in step length of the tilt sensor. The parameter is defined as the ratio between $\alpha_{states,min}$ as the smallest size of the input domain with a constant output value (shortest step) and $\alpha_{states,max}$ for the largest size of the domain (longest step):

$$\xi_{states} = \frac{\alpha_{states,min}}{\alpha_{states,max}}. \tag{2}$$

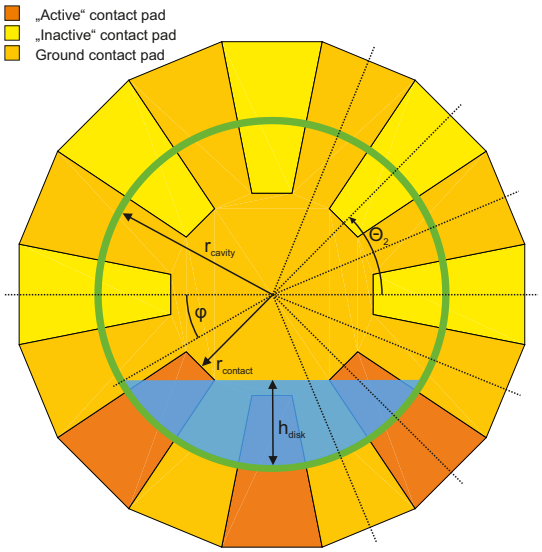

Fig. 6. Representation of parameters for determination of the evaluation parameter ξ_{states} in a tilt sensor with $N = 8$; θ_i is exemplarily depicted for $i = 2$.

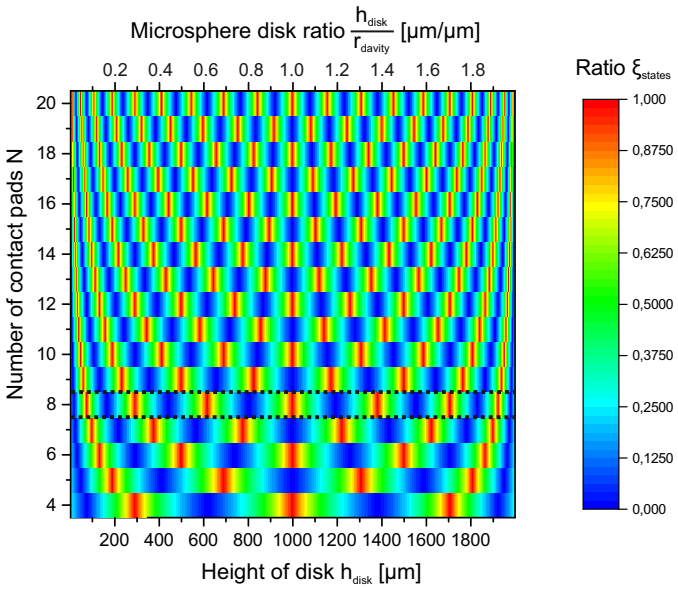

Fig. 7. Evaluation parameter ξ_{states} dependent on the number of contact pads N and the height of the microsphere disk h_{disk}. Contact to ground pad ratio is constant at $\eta_{pad} = 1$, radius of the cavity is $r_{cavity} = 1000\,\mu\text{m}$. The values for $N = 8$ (highlighted by dotted lines) are given in more detail in Fig. 8.

This parameter can assume values between 0 and 1 with $\xi_{states} = 1$ representing the desirable case where all step lengths are identical. In the following, we evaluate the design parameters for their influence on this evaluation parameter ξ_{states}.

Regarding the sensor pad design, the style *No ground* reduces the resolution of the sensor by a factor of 2. Comparing the remaining two styles *Trapezoidal* or *Rectangular*, the former style achieves a better overall value for ξ_{states} when performing a sweep through all other parameters. Therefore, the focus in the following will be on the design *Trapezoidal*.

Both, the inner contact radius $r_{contact}$ and the cavity radius r_{cavity}, do not have any influence on ξ_{states}. Nevertheless, the relation

$$r_{cavity} > r_{contact} + \frac{d_{sphere}}{2} \tag{3}$$

should be kept to ensure that microspheres resting at the edge of the cavity can create an electrical contact with the contact pads below. To define the size of the sensor for the following discussion, we chose $r_{cavity} = 1000\,\mu\text{m}$ and $r_{contacts} = 600\,\mu\text{m}$.

In order to describe the influence of the contact to ground pad ratio η_{pad} as well as the number of microspheres represented by h_{disk}, additional parameters are introduced and exemplarily depicted for an 8-contact tilt sensor in Fig. 6:

The angles θ_i determine the central angles of the contact pads and the ground pads with regard to the horizontal according to:

- for an even number of contact pads N:

$$\theta_i = i * \frac{360°}{2N} \tag{4}$$

with $-\frac{N}{2} + 1 \leq i \leq \frac{N}{2} - 1,\ i \in \mathbb{N}$,

- for an odd number of contact pads N:

$$\theta_i = i * \frac{360°}{2N} + \frac{360°}{4N}. \tag{5}$$

with $-\frac{N-1}{2} \leq i \leq \frac{N-1}{2} - 1,\ i \in \mathbb{N}$.

The angle φ determines the angle between the horizontal and a line drawn from the cavity center to the top edge of the microsphere disk and can be calculated by:

$$\varphi = sin^{-1}\left(\frac{|r_{cavity} - h_{disk}|}{r_{cavity}}\right) \tag{6}$$

Subsequently, the θ_{max} is determined by selecting the θ_i which is closest to φ. Finally, the ratio ξ_{states} is analytically deducted as:

$$\xi_{states} = \frac{min\left\{\left|\varphi - \left(\theta_{max} \pm \frac{360°}{4N}\right)\right|\right\}}{max\left\{\left|\varphi - \left(\theta_{max} \pm \frac{360°}{4N}\right)\right|\right\}} * \mu_{pad} \tag{7}$$

with μ_{pad} as a representation of η_{pad} between 0 and 1:

$$\mu_{pad} = \frac{min\left\{\eta_{pad}; 2 - \eta_{pad}\right\}}{max\left\{\eta_{pad}; 2 - \eta_{pad}\right\}}. \tag{8}$$

With the equations 6 – 8, it is apparent that ξ_{states} depends on N, h_{disk} as well as η_{pad}. In Fig. 7, we show the evaluation parameter for a constant pad ratio $\eta_{pad} = 1$ and varying number of contact pads N and disk heights h_{disk}. As mentioned before, a value of $\xi_{states} = 1$ is aimed, i.e. the red regions are of interest. It can be seen that no single disk height for all number of contacts exists to achieve $\xi_{states} = 1$. Instead, the disk height needs to be selected according to the number of contacts. However, a disk of microspheres that covers half of the cavity, i.e. $h_{disk} = 1000\,\mu\text{m}$, yields a ratio of $\xi_{states} = 1$ for all even N. For odd N, the optimal disk height is always dependent on the number of N and needs to be determined individually for each N.

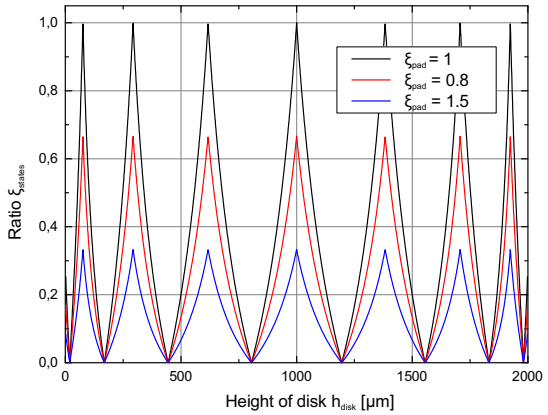

Fig. 8. Evaluation parameter ξ_{states} dependent on the height of the microsphere disk h_{disk} and for different pad ratios η_{pad}, with N = 8.

To determine the amount of microspheres in a disk with a certain height, we first calculate the area of the disk according to [27]

$$\begin{aligned} A_{disk} &= r_{cavity}^2 cos^{-1}\left(\frac{r_{cavity}-h_{disk}}{r_{cavity}}\right) \\ &\quad -(r_{cavity}-h_{disk})\sqrt{2r_{cavity}h_{disk}-h_{disk}^2} \\ &= 1.57\,\mathrm{mm}^2. \end{aligned} \tag{9}$$

with $h_{disk} = 1000\,\mu\mathrm{m}$. With the assumption that the microspheres are densely packed in the plane, the packing density δ_n results in [28]

$$\delta_n = \frac{1}{6}\pi\sqrt{3} \approx 90,7\%. \tag{10}$$

With A_{sphere} as the area of the cross section of the microspheres, we calculate the number of spheres as

$$N_{spheres} = \left\lceil \frac{\delta_n \cdot A_{disk}}{A_{sphere}} \right\rceil = 29 \tag{11}$$

that are needed to fill a planar disk with the height of $1000\,\mu\mathrm{m}$.

To evaluate the influence of η_{pad}, the results of Fig. 7 are shown in more detail for $N = 8$ and different values of η_{pad} in Fig. 8. It is evident, also from Eq. 7, that any value $\eta_{pad} \neq 1$ decreases the value of ξ_{states} and leads to an increased nonlinearity. The angular width of the contact pads and the ground pads should therefore have the same value, independent of the height of the microsphere disk h_{disk}.

The above discussion shows that the performance of the tilt sensor mainly depends on the number of contact pads as well as the number of microspheres. For the following section V we define all parameters as follows:

1) *Number of contact pads*: $N = 8$, achieving $\alpha_{res} = 22.5°$
2) *Sensor pad design*: Trapezoidal
3) *Inner contact radius*: $r_{contact} = 600\,\mu\mathrm{m}$
4) *Radius of sensor cavity*: $r_{cavity} = 1000\,\mu\mathrm{m}$
5) *Ratio of ground to contact pad*: $\eta_{pad} = 1$
6) *Amount of microspheres*: $N_{spheres} = 29$.

Based on these parameters, Fig. 9 shows a macrograph of the assembled tilt sensor with the connection pads as well as a micrograph with the microspheres loaded in the cavity.

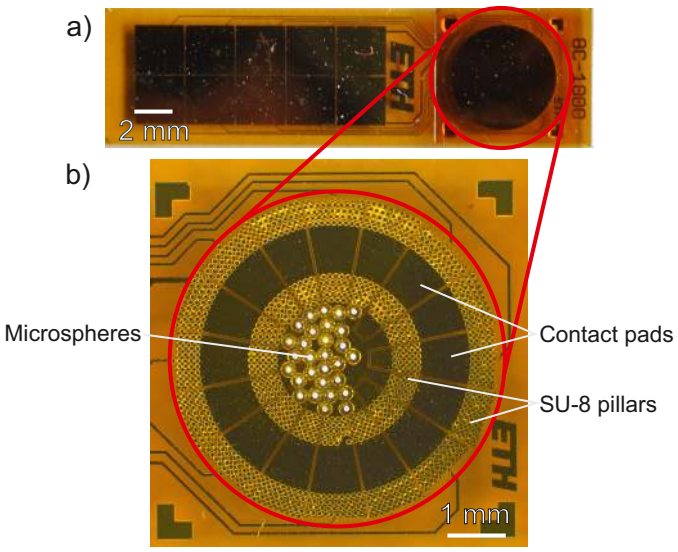

Fig. 9. (a) Macrograph of final assembled tilt sensor with 8 contact pads including connection pads; (b) Macrograph of tilt sensor cavity before closure of cavity.

The sensing structure has a height of $400\,\mu\mathrm{m}$ (including the substrate).

V. Characterization

We now evaluate the characteristics of the sensor. First, we introduce the characterization setup along with the definition of required dimensions before we investigate the static behavior of the tilt sensor. Finally, the response time of the sensor due to the microsphere movement is evaluated.

A. Experimental setup and definitions

The tilt of the sensor is described by two angles according to Fig. 10b. The normal of the sensor plane of the tilt sensor is tilted by the angle β with regard to the vertical. Then, the tilt sensor is rotated by the angle α around the normal of the sensor plane. This is the angle which is the measurement value α of the tilt sensor.

We characterize the static response of the tilt sensor with a tilt table with two axes. The tilt table is shown in Fig. 10a with an identification of the two axes. The tilt table is electronically controlled by a PC and can run curves where the tilt of the sensor plane β is fixed and only the sensor tilt α is changed. A data logger is connected to each contact pad of the tilt sensor and measures the contact resistance between each contact pad and the ground plane of the tilt sensor with a current of $1\,\mathrm{mA}$. Finally, the PC uses the respective look-up table, e.g. Tab. I, to determine the measured tilt by the tilt sensor.

B. Static evaluation

The movement of microspheres inside the cavity of the tilt sensor exhibits a hysteresis, i.e. not every change in the tilt angle α leads to an immediate change in the position of the microspheres. Only once a threshold angle α_{hys} is reached, the microspheres start rolling towards gravity and take a new position at the bottom of the cavity.

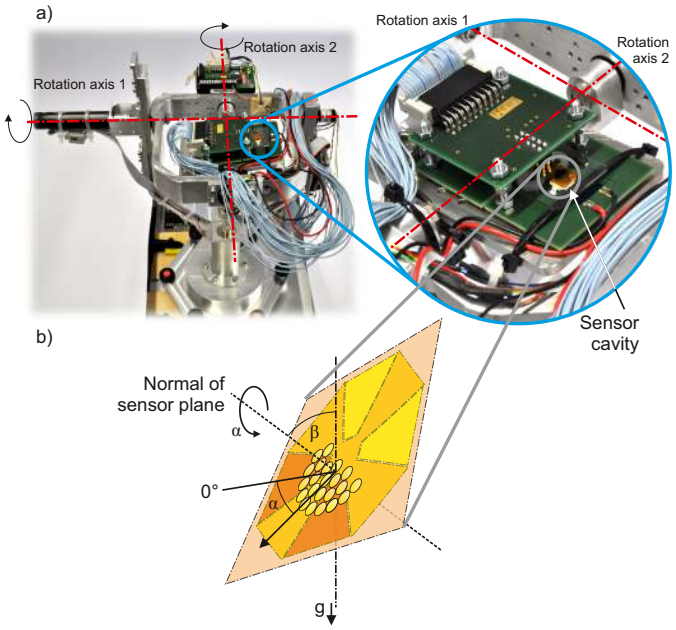

Fig. 10. (a) Photograph of the sensor characterization tilt table with identification of the two rotation axes and a close-up (right) of the tilt sensor; (b) Schematic of the tilt sensor with identification of two tilt angles.

We record the hysteresis angle α_{hys} at which the microspheres start moving to a new position while rotating the tilt sensor at a given, constant angle β. As values for α_{hys} are smaller than the angular resolution of $22.5°$ of the tilt sensor, the change of position of the microspheres is determined by visual observation of the microspheres inside the cavity. We repeat the measurement several times for each sensor plane tilt β and depict the average and standard deviation of the resulting hysteresis angle in Fig. 11.

The tilt of the sensor plane β has an influence on the hysteresis angle: the hysteresis angle as well as its standard deviation decrease with increasing tilt of the sensor plane. For $\beta \geq 50°$, α_{hys} is constant at $10°$ with a minimal standard deviation of $2°$.

The movement of the microspheres in the cavity is composed of rolling as well as sliding. The gravitational force which acts on the microspheres in the cavity is the main force for both effects and is proportional to $sin(\beta)$. Thus, α_{hys} is large for small tilt angles of the sensor plane. The dominating cause which initiates the movement of the microsphere bulk is a single microsphere which starts rolling and then causes an avalanche of all. However, as the arrangement of the microspheres is - to some degree - random, the standard deviation is large for small β.

It is desirable to operate the tilt sensor with a hysteresis as low as possible, i.e. the tilt sensor should be operated at an angle $90° > \beta \geq 50°$. As the weight and pressure of the microspheres onto the contact pads is reduced for a tilt of the sensor plane close to vertical ($90°$), the electrical contact is reduced and not reliable. Thus, the sensor is characterized at a tilt of $50°$ in the following to balance the hysteresis as well as the reliability of the electrical contact.

Fig. 12 shows the sensor output with respect to the applied

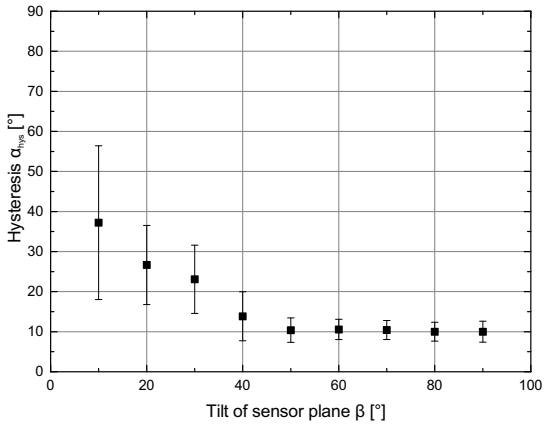

Fig. 11. Hysteresis α_{hys} of the tilt sensor (i.e. movement of the microspheres) at different tilt angles of the sensor plane β.

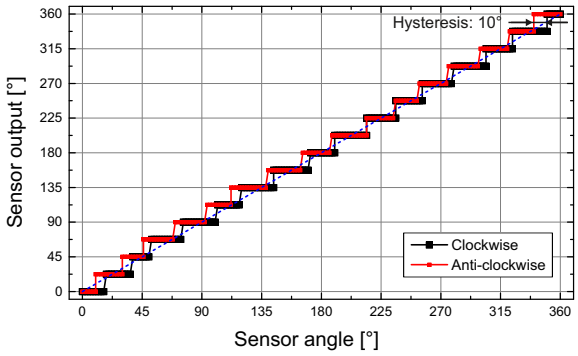

Fig. 12. Characteristics of a 8-contact tilt sensor at a tilt of the sensor plane $\beta = 50°$.

sensor angle α for a clockwise as well as anti-clockwise response. Again, we observe a hysteresis of $10°$ between both curves which is comparable to the hysteresis depicted in Fig. 11. The sensor response follows the bisecting line. However, small non-linearities can be observed. These can be attributed to the randomness of the microsphere arrangement as well as the fact that the microspheres are not ideally densely packed inside the cavity (as can be seen in Fig. 9).

C. Response time

While at a tilt of $\beta = 50°$, the sensor was rotated with a rotational speed of $50\,°\,\mathrm{s}^{-1}$ in order to gain an understanding on the movement of the microspheres and its time scale. The microsphere movement was recorded with a high-speed camera (*Phantom v1610*) at a frame rate of $1000\,\mathrm{fps}$. Instead of using a gold coated polyimide layer, the cavity was sealed with a glass slide covered with conductive indium tin oxide (ITO) to ensure a good visibility of the microspheres. The transparent ITO was connected to the ground contact of the sensor and thus mitigated the build up of electrostatic charges that could hinder the microsphere movement.

From the recording which is shown in excerpts in Fig. 13a the response time, i.e. time scale of movement, is $53\,\mathrm{ms}$. This is the time from when the microspheres start moving inside the cavity until they come to a rest. The video recording also shows that the movement of the microspheres is initiated by

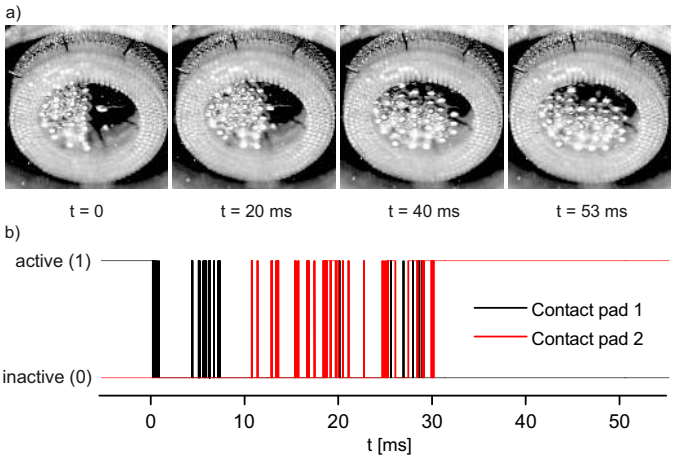

Fig. 13. (a) High-speed recording of microsphere movement inside cavity at $\beta = 50°$; (b) Electrical response of two contacts pads which change their state during the movement of microspheres.

a single microsphere which starts rolling and then causes an avalanche of the bulk of microspheres. During this time of $53\,\mathrm{ms}$, the cavity rotates less $3°$.

We confirm this time frame by recording the electrical response of the tilt sensor with an oscilloscope (Fig. 13b). Here, we observe a response time of less than $31\,\mathrm{ms}$ which indicates that the microspheres already create an electrical connection while they are still moving inside the cavity. During the movement of the microspheres, the state of the contact pad on which the microspheres are rolling across oscillates randomly between *active* and *inactive*. This leads to output combinations of the tilt sensor that do not correspond to an entry in the look-up table. Therefore, use of the tilt sensor is only possible in static applications as dynamic operation can lead to measurement artefacts.

VI. Conclusion

We presented a novel type of flexible tilt sensor where conductive microspheres act as the pendulum. The microspheres are placed inside a cavity which side walls are defined by SU-8 pillars, whereas the top and the bottom layer of the sensor are made of flexible polyimide foil. Patterned metal contacts on the substrate allow identifying the position of the microspheres and thus relating back to the orientation of the tilt sensor. In this work, we exemplarily presented a tilt sensor with 8 contacts, achieving an angular resolution of $22.5°$ and a hysteresis of below $10°$.

By modeling the sensor, we identified the design parameters which influence the sensor performance, such as resolution and non-linearity. The number of microspheres inside the cavity along with the number of contact pads are the most important parameters and need to be selected according to the desired needs. In addition the tilt of the sensor plane β was found to have an influence on the hysteresis and therefore the sensor should best be operated at a sensor plane tilt of $50°$. Recordings of the microsphere movements conclude a sensor response time of $\sim 50\,\mathrm{ms}$, therefore rendering the sensor useful mainly for more static applications. By using two or more tilt sensors in different orientations, it can be determined whether the tilt of the plane of a specific sensor is around $50°$ and whether the output values of this specific sensor are reliable.

Based on the simple readout principle, a wireless readout of the sensor without an own power supply on the sensor could be envisioned. This would be a step forward for the development of wearable electronics, as the power supply of these devices is still one of the limiting factor for a breakthrough. In addition, more complex cavity designs than just circular are possible, which would allow to adapt the sensor to specific applications, e.g. an electronic version of a TiltWatch [29] which is used in shipping and handling monitoring.

Acknowledgment

This work was supported by the EU Marie Curie Network iCareNet under grant number 264738. The authors would like to thank Jinwoong Cha for his assistance with the high-speed recording of the microsphere movements.

References

[1] Gartner, "Gartner says worldwide wearable devices sales to grow 18.4 percent in 2016," accessed 17.09.2016, Feb. 2016. [Online]. Available: http://www.gartner.com/newsroom/id/3198018

[2] K. Cherenack, C. Zysset, T. Kinkeldei, N. Münzenrieder, and G. Tröster, "Wearable electronics: Woven electronic fibers with sensing and display functions for smart textiles," *Advanced Materials*, vol. 22, no. 45, p. 5071, 2010.

[3] N. Münzenrieder, L. Petti, C. Zysset, D. Görk, L. Büthe, G. Salvatore, and G. Tröster, "Investigation of gate material ductility enables flexible a-igzo tfts bendable to a radius of 1.7 mm," in *Solid-State Device Research Conference (ESSDERC), 2013 Proceedings of the European*, 2013, pp. 362–365.

[4] K. Song, J. Noh, T. Jun, Y. Jung, H.-Y. Kang, and J. Moon, "Fully flexible solution-deposited zno thin-film transistors," *Advanced Materials*, vol. 22, no. 38, pp. 4308–4312, 2010.

[5] Y. Moser and M. Gijs, "Miniaturized flexible temperature sensor," *Microelectromechanical Systems, Journal of*, vol. 16, no. 6, pp. 1349–1354, 2007.

[6] S. C. Mannsfeld, B. C. Tee, R. M. Stoltenberg, C. V. H. Chen, S. Barman, B. V. Muir, A. N. Sokolov, C. Reese, and Z. Bao, "Highly sensitive flexible pressure sensors with microstructured rubber dielectric layers," *Nature materials*, vol. 9, no. 10, pp. 859–864, 2010.

[7] T. Kinkeldei, C. Zysset, N. Münzenrieder, and G. Tröster, "An electronic nose on flexible substrates integrated into a smart textile," *Sensors and Actuators B: Chemical*, vol. 174, pp. 81–86, 2012.

[8] H. Harms, O. Amft, G. Tröster, and D. Roggen, "Smash: A distributed sensing and processing garment for the classification of upper body postures," in *Proceedings of the ICST 3rd International Conference on Body Area Networks*, ICST, Brussels, Belgium, Belgium, 2008, pp. 22:1–22:8.

[9] I. Gönenli, Z. Celik-Butler, and D. Butler, "Surface micromachined mems accelerometers on flexible polyimide substrate," *Sensors Journal, IEEE*, vol. 11, no. 10, pp. 2318 –2326, oct. 2011.

[10] T. G. Constandinou and J. Georgiou, "Micro-optoelectromechanical tilt sensor," *Journal of Sensors*, 2008.

[11] J. C. Choi, Y. C. Choi, J. K. Lee, and S. H. Kong, "Miniaturized dual-axis electrolytic tilt sensor," *Japanese Journal of Applied Physics*, vol. 51, no. 6, p. 06FL13, 2012.

[12] J. Courteaud, P. Combette, N. Crespy, G. Cathebras, and A. Giani, "Thermal simulation and experimental results of a micromachined thermal inclinometer," *Sensors and Actuators A: Physical*, vol. 141, no. 2, pp. 307 – 313, 2008.

[13] L. Tang, K. Zhang, S. Chen, G. Zhang, and G. Liu, "MEMS inclinometer based on a novel piezoresistor structure," *Microelectronics Journal*, vol. 40, no. 1, pp. 78 – 82, 2009.

[14] H. Ueda, H. Ueno, K. Itoigawa, and T. Hattori, "Micro capacitive inclination sensor utilizing dielectric nano-particles," in *Micro Electro Mechanical Systems, 2006. MEMS 2006 Istanbul. 19th IEEE International Conference on*, 2006, pp. 706–709.

[15] B. Ando, A. Ascia, and S. Baglio, "A ferrofluidic inclinometer in the resonant configuration," *Instrumentation and Measurement, IEEE Transactions on*, vol. 59, no. 3, pp. 558–564, 2010.
[16] J.-H. Wu, K.-Y. Horng, S.-L. Lin, and R.-S. Chang, "A two-axis tilt sensor based on optics," *Measurement Science and Technology*, vol. 17, no. 4, p. N9, 2006.
[17] L. Amaral, O. Frazao, J. Santos, and A. Ribeiro, "Fiber-optic inclinometer based on taper michelson interferometer," *Sensors Journal, IEEE*, vol. 11, no. 9, pp. 1811–1814, Sept 2011.
[18] L. Rovati and S. Cattini, "Contactless two-axis inclination measurement system using planar flux-gate sensor," *IEEE Transactions on Instrumentation and Measurement*, vol. 59, no. 5, pp. 1284–1293, May 2010.
[19] L. Büthe, C. Vogt, L. Petti, N. Münzenrieder, C. Zysset, G. A. Salvatore, and G. Tröster, "A mechanically flexible tilt switch on kapton foil with microspheres as a pendulum," in *Sensors and Measuring Systems 2014; 17. ITG/GMA Symposium; Proceedings of*, 2014, pp. 1–4.
[20] M. Tariq, M. G. Freire, B. Saramago, J. A. P. Coutinho, J. N. C. Lopes, and L. P. N. Rebelo, "Surface tension of ionic liquids and ionic liquid solutions," *Chem. Soc. Rev.*, vol. 41, pp. 829–868, 2012.
[21] M. J. Earle, J. M. Esperança, M. A. Gilea, J. N. C. Lopes, L. P. Rebelo, J. W. Magee, K. R. Seddon, and J. A. Widegren, "The distillation and volatility of ionic liquids," *Nature*, vol. 439, no. 7078, pp. 831–834, 2006.
[22] R. A. Wydro Sr, "Method of producing solder spheres," Apr. 19 1983, uS Patent 4,380,518.
[23] W. E. Elsholz, "Fabrication of glass microspheres with conducting surfaces," US Patent 4,459,145, 1984.
[24] S. McAllister, S. Patankar, I. F. Cheng, and D. Edwards, "Lead dioxide coated hollow glass microspheres as conductive additives for lead acid batteries," *Scripta Materialia*, vol. 61, no. 4, pp. 375 – 378, 2009.
[25] J.-H. Lee, B. C. Moon, J. Lee, J.-T. Moon, C.-R. Oh, and J. G. Nam, "Method of manufacturing solder balls," US Patent 6,312,498, 2001.
[26] U. Tietze, C. Schenk, and E. Gamm, *Electronic circuits: handbook for design and application*. Springer, 2015.
[27] E. Weisstein, "Circular segment - mathworld - a wolfram web resource," accessed 17.09.2016. [Online]. Available: http://mathworld.wolfram.com/CircularSegment.html
[28] J. H. Conway and N. J. A. Sloane, *Sphere packings, lattices and groups*. Springer Science & Business Media, 2013, vol. 290.
[29] Schockwatch, "Tilt indicators - shipping and handling monitoring devices," accessed 17.09.2016. [Online]. Available: http://shockwatch.com/products/impact-and-tilt/tilt-indicators

Lars Büthe (S'13) received the diploma degree in mechatronics from the University of Erlangen-Nuremberg, Erlangen, Germany, and a master of technology management from the University of New South Wales, Sydney, Australia. In 2017, he graduated with a Ph.D. degree from the Swiss Federal Institute of Technology (ETH) Zurich, Zurich, Switzerland.

His current research interests include flexible electronics and sensors.

Christian Vogt (S'14) received the M.Sc. degree in electrical engineering and information technology from the Swiss Federal Institute of Technology (ETH) Zurich in 2013. Since 2013 he has been pursuing the Ph.D. degree with the Swiss Federal Institute of Technology (ETH) Zurich, Zurich, Switzerland.

His current research interests include flexible electronics and applications for magnetic resonance imaging.

Luisa Petti (S'12) received the M.Sc. degree in electronic engineering from Politecnico di Milano in 2011, and the Ph.D. degree in electrical engineering and information technology from Swiss Federal Institute of Technology (ETH) Zurich in 2016.

Her current research interests are the development, fabrication, and characterization of flexible thin-film devices based on metal oxide semiconductors.

Giuseppe Cantarella received the M.Sc degree in electronic engineering from Polytechnic of Turin, Turin, Italy, in 2013. Since 2013, he has been pursuing the Ph.D. degree with the Swiss Federal Institute of Technology (ETH) Zurich, Zurich, Switzerland.

His current research interests include flexible electronics.

Niko Münzenrieder (M'14) received a diploma in physics from the Technical University Munich in 2008, and a Ph.D. in electrical engineering from the Swiss Federal Institute of Technology Zurich in 2013.

Currently he is a lecturer at the University of Sussex working on flexible and stretchable thin-film electronics.

Gerhard Tröster has been a full professor of electronics with the Swiss Federal Institute of Technology Zurich, Zurich, Switzerland, since 1993.

His current research interests include signal processing, wireless sensor networks, wearable computing, smart textiles applying flexible, and organic electronics.